Chang, S. P., Brown, M., & Rittenberg, M. B. (1982) *J. Immunol. 128*, 702.
Clore, G. M., & Gronenborn, A. M. (1982) *J. Magn. Reson. 48*, 402.
Ernst, R. R., Bodenhausen, G., & Wokaun, A. (1987) *Principles of Nuclear Magnetic Resonance in One and Two Dimensions*, Clarendon, Oxford.
Glaudemans, C. P. J., Lerner, L., Daves, G. D., Jr., Kováč, P., Venable, R., & Bax, A. (1990) *Biochemistry 29*, 10906.
Keepers, J. W., & James, T. L. (1984) *J. Magn. Reson. 57*, 404.
Koide, S., Yokoyama, S., Matsuzawa, H., Miyazawa, T., & Ohta, T. (1989) *J. Biol. Chem. 264*, 8676.
Kumar, A., Ernst, R. R., & Wüthrich, K. (1980) *Biochem. Biophys. Res. Commun. 95*, 1.
Marion, D., & Wüthrich, K. (1983) *Biochem. Biophys. Res. Commun. 113*, 967.
Price, W. J. (1972) in *Laboratory Methods in Infrared Spectroscopy* (Miller, R. G. J., & Stace, B. C., Eds.) 2nd ed., p 115, Heydon and Sons, London.
Pullman, B., Berthod, H., & Gresh, N. (1975) *FEBS Lett. 53*, 199.
Richard, H., Dufourcq, J., & Lussan, C. (1974) *FEBS Lett. 45*, 136.
Satow, Y., Cohen, G. H., Padlan, E. A., & Davies, D. R. (1986) *J. Mol. Biol. 190*, 593.
Segal, D. M., Padlan, E. A., Cohen, G. H., Rudikoff, S., Potter, M., & Davies, D. R. (1974) *Proc. Natl. Acad. Sci. U.S.A. 71*, 4298.
Stenzel-Poore, M. P., & Rittenberg, M. B. (1989) *J. Immunol. 143*, 4123.
Zilber, B., Scherf, T., Levitt, M., & Anglister, J. (1990) *Biochemistry 29*, 10032.

Role of Glucose Carrier in Human Erythrocyte Water Permeability†

Mark L. Zeidel,*,‡ Ariela Albalak,‡ Eric Grossman,‡ and Anthony Carruthers§
Department of Medicine, West Roxbury Veterans Administration Medical Center, Brigham and Women's and Children's Hospitals, Harvard Medical School, 1400 V.F.W. Parkway, West Roxbury, Massachusetts 02132, and Department of Biochemistry and Molecular Biology and Program in Molecular Medicine, University of Massachusetts Medical School, 373 Plantation Street, Worcester, Massachusetts 01605

Received June 19, 1991; Revised Manuscript Received September 24, 1991

ABSTRACT: Although the transport properties of human erythrocyte water channels have been well characterized, the identity of the protein(s) mediating water flow remains unclear. Recent evidence that glucose carriers can conduct water raised the possibility that the glucose carrier, which is abundant in human erythrocytes, is the water channel. To test this possibility, water permeabilities and glucose fluxes were measured in large unilamellar vesicles (LUV) containing human erythrocyte lipid alone (lipid LUV), reconstituted purified human erythrocyte glucose carrier (Glut1 LUV), or reconstituted glucose carrier in the presence of other human erythrocyte ghost proteins (ghost LUV). In glucose and ghost LUV, glucose carriers were present at 25% of the density of native erythrocytes, were oriented randomly in the bilayer, and exhibited characteristic inhibition of glucose flux when exposed to cytochalasin B. Osmotic water permeability (P_f, in centimeters per second; $n = 4$) averaged 0.0012 ± 0.00033 in lipid LUV, 0.0032 ± 0.0015 in Glut1 LUV, and 0.006 ± 0.0014 in ghost LUV. Activation energies of water flow for the three preparations ranged between 10 and 13 kcal/mol; *p*-(chloromercuri)benzenesulfonate (pCMBS), an organic mercurial inhibitor of erythrocyte water channels, and cytochalasin B did not alter P_f. These results indicate that reconstitution of glucose carriers at high density increases water permeability but does not result in water channel activity. However, because the turnover number of reconstituted carriers is reduced from that of native carriers, experiments were also performed on erythrocyte ghosts with intact water channel function. In ghosts, P_f averaged 0.038 ± 0.013 ($n = 9$), while the activation energy for water flow averaged 3.0 ± 0.3 kcal/mol. Mercuric chloride reduced P_f by 93%, while pCMBS reduced it by 69%. Thus, ghosts retained water channel function. Preparation of ghosts in the presence of calcium led to markedly reduced glucose carrier activity without altering P_f. In addition, cytochalasin B did not reduce P_f. We conclude that the erythrocyte glucose carrier is not the water channel. The identity of the erythrocyte water channel remains elusive.

Although numerous transport studies have characterized the activity of a water channel in the plasma membrane of the human erythrocyte, the identity of this channel remains unclear (Macey, 1984; Finkelstein, 1986; Solomon, 1972). Estimates based on the high water permeability of erythrocyte plasma membranes suggest that each erythrocyte contains approximately 10^6 water channels (Finkelstein, 1986). These considerations suggest that proteins present in erythrocyte membranes in high density, such as the anion exchanger and the glucose carrier, are prime candidates to function as water channels (Macey, 1984; Finkelstein, 1986). Although the anion exchange protein is the most abundant membrane protein in the erythrocyte, several studies have dissociated

† Supported by NIH Grant RO-1 DK36081 awarded to A.C. and NIH Grant RO-1 DK43955 awarded to M.L.Z. M.L.Z. is the recipient of Research Career Development and Merit Review Awards from the Department of Veterans Affairs.
* Address correspondence to this author at Research Service, West Roxbury Veterans Administration Medical Center, 1400 V.F.W. Parkway, West Roxbury, MA 02132.
‡ West Roxbury Veterans Administration Medical Center, Brigham and Women's and Children's Hospitals, and Harvard Medical School.
§ University of Massachusetts Medical School.

0006-2960/92/0431-589$03.00/0

water flux and anion exchange, suggesting that distinct structures mediate these activities (Macey, 1984; Finkelstein, 1986). Thus, stilbenes inhibit anion exchange without altering water flow, and organic mercurials such as *p*-chloromercuribenzenesulfonate (pCMBS) inhibit water flow without altering anion exchange. In addition, avian erythrocytes exhibit active anion exchange but lack water channel function (Macey, 1984).

Several lines of evidence suggest that the glucose carrier may also function as the erythrocyte water channel: (1) Organic mercurial compounds such as pCMBS inhibit both water flow and glucose transport (Macey, 1984; Carruthers, 1990). (2) Avian erythrocytes lack both water channels and mediated glucose transport (Macey, 1984; Carruthers, 1990). (3) Infrared spectroscopy of reconstituted glucose carriers has provided suggestive evidence that a large proportion of the protein is accessible to deuterium for exchange, consistent with the presence of a pore capable of conducting water (Alvarez et al., 1987; Jung et al., 1986). (4) Measurements of osmotic water flow in J774 macrophages have demonstrated that inhibitors of mediated glucose transport such as cytochalasin B, tometin, and phloretin, but not the inactive dihydrocytochalasin B, reduce water flow with potency similar to that obtained in measurements of glucose flux (Fischbarg et al., 1989). (5) Injection of glucose transporter mRNA into *Xenopus* oocytes results in increased water permeability; extrapolations from the permeability data suggest that glucose carriers increased oocyte water permeability sufficiently for these carriers to account for water flux in intact erythrocytes (Fischbarg et al., 1990).

The present studies were designed to test the hypothesis that the erythrocyte glucose carrier is responsible for a significant portion of water channel mediated water flux in human erythrocytes. Glucose carrier and other erythrocyte proteins were reconstituted into lipid bilayers, and the activity of water channels was assayed. In addition, the relationship between glucose and water transport was examined in erythrocyte ghosts with intact water channel function.

Materials and Methods

Materials. [^{3}H]Cytochalasin B, D-[^{14}C]glucose, 3-*O*-[^{14}C]methylglucose, [^{14}C]inulin, and ^{125}I-labeled protein A were purchased from New England Nuclear. Rabbit antisera raised against a synthetic carboxy-terminal peptide of Glut1 (intracellular residues 480–492; C-IgGs) were obtained from East Acres Biologicals. Anti-Glut1 antisera reacting exclusively with an extracellular moiety of Glut1 (δ-IgGs) were prepared as described previously (Harrison et al., 1990). Carboxyfluorescein, chromatographically purified, was obtained from Molecular Probes, Junction City, OR. Anti-fluorescein antibody was prepared as described (Harris et al., 1990b). All other chemicals were obtained from Sigma, St. Louis, MO, and were of analytical grade.

Solutions. Saline solution consisted of 150 mM NaCl, 5 mM Tris-HCl, and 0.2 mM EDTA, pH 7.4. Phosphate-buffered saline consisted of 50 mM sodium phosphate/100 mM NaCl, pH 8.0. Lysis medium contained 10 mM Tris-HCl/2 mM EDTA, pH 7.4. Tris medium consisted of 50 mM Tris-HCl/02. mM EGTA, pH 7.4. KCl medium consisted of 20.75 mM sucrose, 7.5 mM KCl, 7.5 mM K-HEPES, and 0.1 mM EDTA, pH 8.0, with a measured osmolality of 50 ± 2 mOsm/kg.

Erythrocyte Ghost Preparations for Flux Studies. Fresh blood (6 mL) drawn into 0.1 mL of 6 mM EDTA was diluted 1:10 with phosphate-buffered saline and washed 3 times by centrifuging at 12000*g* for 5 min. Final pellets were diluted into 120 mL of 5 mM sodium phosphate buffer, pH 8.0, and washed 3 times at 50000*g* for 10 min. At the end of each spin, the supernatant and white blood cell pellets were removed. After the final wash, the membranes were resuspended in 5 mM sodium phosphate, pH 8.0, containing 0.1 mM EDTA and centrifuged at 50000*g* for 10 min. The pellet was then resuspended in 10 mL of KCl medium containing 20 mM carboxyfluorescein in the presence or absence of 1 mM $CaCl_2$ and incubated for 40 min at 37 °C. Ghosts were then washed 6–10 times in water flow buffer (50000*g* for 10 min) until extravesicular fluorescence (determined by the effect of adding extravesicular anti-fluorescein antibody) was minimal.

Reconstitution of Ghost Proteins and Purified Glucose Carrier into Large Unilameller Vesicles Red cell ghosts were prepared from washed red cells as in Helgerson et al. (1989) and were depleted of peripheral membrane proteins by a single alkali wash as in Carruthers (1986). Glut1 plus endogenous lipid was purified from human erythrocytes as described by Cairns et al. (1984). Red cell lipids were extracted from red cell ghosts or from purified Glut1 by the method described in Helgerson et al. (1989). Detergent extracts of red cell ghost membranes, of purified Glut1, or of lipid extracts of purified Glut1 were reconstituted into egg phosphatidylcholine (EPC) bilayers by cholate dialysis. EPC (30 mg in hexane) was dried to a thin film under N_2. The lipid film was placed in vacuo for 3 h to remove traces of remaining solvent. The lipid was dissolved in 2 mL of KCl buffer plus 32 mg of cholic acid (the minimum amount found necessary to solubilize this amount of EPC) and centrifuged at 34000*g* for 30 min, and the supernatant was placed on ice. Glut1 (10–100 μg), total membrane protein containing 10–100 μg of Glut1 protein, or lipid extracted from sufficient red cell membranes (500–5000 μg) to yield 10–100 μg of Glut1 was dissolved in KCl buffer containing 50 mM cholic acid (cholate:lipid molar ratio = 2) by end-over-end rotation at 5 °C for 30 min. The sample was centrifuged at 34000*g* for 30 min, and the supernatant was combined with the solubilized EPC and mixed by end-over-end rotation at 5 °C for 30 min. The lipid–protein mixture was dialyzed against two changes of 6 L of saline at 5 °C for 24 h. The resulting small unilamellar proteoliposomes were mixed with 1 volume of carboxyfluorescein (40 mM in KCl buffer, pH 8.0). The suspension was frozen rapidly in dry ice/acetone and then allowed to thaw at room temperature. The resulting proteoliposomes were large (1–3 μm in diameter as judged by phase-contrast microscopy) and were sedimented by centrifugation at 14000*g* for 5 min.

LUV diameters were assessed by phase-contrast light microscopy and by laser scattering (Coulter Submicron particle analyzer), with close agreement between the two methods. Pearson V distribution function analysis of the correlation coefficients resulted in polydispersity factors of 0.1 or less, indicating substantially monodispersed samples (Carruthers & Melchior, 1984).

Encapsulated Volumes. The encapsulated volumes of proteoliposomes were measured by addition of [^{14}C]inulin to the suspension of small unilamellar proteoliposomes prior to the freeze–thaw step. Following fusion to form large proteoliposomes, the proteoliposomes were sedimented by centrifugation, samples of the supernatant were counted, and the proteoliposomes were washed at least 5 more times until the supernatant counts were reduced to background levels. The proteoliposomes were dissolved in SDS (0.5%) and assayed for phospholipid phosphorus and [^{14}C]inulin.

Glucose Carrier Orientation in Proteoliposomes. The orientation of Glut1 in reconstituted proteoliposomes was estimated using C- and δ-IgGs. Two methods were used. In ELISA assays, the amount of immunoreactive material present in Triton X-100 permeabilized and Triton X-100 free proteoliposomes was assayed. These measurements permit the determination of the fraction of total Glut1 that presents either external or internal epitopes to the exterior of proteoliposomes. In other experiments, the extent of IgG binding to 10-μL aliquots of proteoliposomes was determined using ^{125}I-protein A (Harrison et al., 1990). Purified Glut1 was used as an internal standard. C- and δ-IgGs have access to cytoplasmic and extracellular domains, respectively, of purified Glut1. Binding of IgG to proteoliposomes (excess IgG levels were employed) was expressed as a fraction of the binding detected using an equal aliquot of purified Glut1. The assumption with this approach is that Glut1 is uniformly distributed among all proteoliposomes (i.e., the Glut1:phospholipid ratio of all proteoliposomes is identical). Evidence supporting this assumption is presented below.

Sugar Transport Assays in Red Cell Ghosts and Proteoliposomes. α-D-[U-^{14}C]Glucose uptake at 0.1 mM D-glucose ± 10 μM cytochalasin B by reconstituted proteoliposomes at 20 °C and 0.1 mM 3-*O*-[^{14}C]methylglucose uptake by ghosts at ice temperature were assayed as described previously (Helgerson et al., 1989; Hebert & Carruthers, 1991).

Measurement of Water Permeability. Osmotic water flow was measured by monitoring the self-quenching of entrapped carboxyfluorescein (CF; Harris et al., 1990a). At high concentrations, CF self-quenches. In vesicles containing entrapped CF at high concentration, extravesicular osmolality was raised, resulting in efflux of water from the vesicles, an increase in intravesicular CF concentration, and further self-quenching of entrapped CF. To measure intravesicular fluorescence, sufficient extravesicular anti-fluorescein antibody was added to quench extravesicular fluorescence. By measurement of intravesicular fluorescence in the presence of increasing levels of extravesicular osmolality, the relationship between relative vesicle volume and relative fluorescence was obtained. Standard curves relating the relative fluorescence to relative volume were obtained on an SLM-Aminco 500C spectrofluorometer (excitation, 490; nm; emission, 525 nm). Over the range of osmolalities employed in the stopped-flow experiments (initial internal osmolality, 50 mOsm/kg; initial external osmolality, 100–200 mOsm/kg) relative fluorescence was a linear function of relative volume [correlation coefficients (R) were greater than 0.95]. This linear relationship was also obtained in measurements acquired using the stopped-flow device. In all experiments, external solutions contained sufficient anti-fluorescein antibody to quench all external carboxyfluorescein fluorescence.

Water flow measurements were performed on an Applied Photophysics SF.17 MV stopped-flow spectrofluorometer with a measured dead time of 0.7 ms, a mixing chamber volume of 20 μL, and injection volumes of 50 μL from each syringe. The excitation wavelength was 490 nm, and emitted light was filtered with a 515-nm cutoff filter. Vesicles or ghosts were placed in one drive syringe, and hypertonic or isotonic solution was placed in the other drive syringe. For all experiments, control runs were performed by mixing vesicles or ghosts into a buffer solution identical to the one in which they were suspended. To enhance the signal to noise ratio, 5–10 curves for each experiment were averaged. Averages of control runs (vesicles or ghosts mixed into buffer) were subtracted from averaged runs mixing vesicles or ghosts with hypertonic solutions. Fluorescence data were fitted to single exponentials using the software accompanying the Applied Photophysics instrument on a RISC-based Archimedes computer. The software utilizes a nonlinear regression (Marquardt) algorithm based on the "Curfit" routine in Bevington (1969). P_f was calculated from the time course of relative fluorescence by comparing single-exponential time constants fitted to the fluorescence data with single-exponential time constants fitted to simulated curves in which P_f was varied. Simulated curves were calculated using a commercially available software package (MathCad) from the osmotic permeability equation and the relation between relative flurorescence and relative volume:

$$d[V_{(t)}]/dt = P_f(SAV)(MVW)[C_{in.(t=0)}/V(t) - C_{out}] \quad (1)$$

where $V_{(t)}$ is the relative volume of the vesicles at time t (i.e., the absolute volume divided by the inital volume), SAV is the surface area to volume ratio, MVW is the molar volume of water (18 cm^3/mol), $C_{in.(t=0)}$ is the initial intravesicular osmolarity, and C_{out} is the extravesicular osmolality (Illsley & Verkman, 1986). Since the volume within vesicles or ghosts was small compared with the volume outside, it was assumed that C_{out} remained constant throughout the experiment. Parameters from the exponential fit (amplitude and end point) were used to relate relative fluorescence to relative volume using the boundary assumptions that relative fluorescence and volume are 1.0 at time zero and that relative volume reaches a known value (if the osmolality outside is double that inside, relative volume reaches 0.5) at the end of the experiment while relative fluorescence reaches the values obtained from the fitted curve. Single-exponential fits of fluorescence data have been used to determine P_f in a number of membranes (Illsley & Verkman, 1986; Chen et al., 1988; Meyer & Verkman, 1986), including erythrocyte ghosts (Harris et al., 1990a), because curves derived from eq 1 do not deviate significantly from single exponentials. In addition, it can be shown mathematically that at earlier time points eq 1 approximates a first-order process (Harris et al., 1990a). SAV was measured by determining the diameters of the vesicles or ghosts under phase-contrast microscopy and a light-scattering device; vesicles and ghosts appeared to be spherical under phase-contrast microscopy.

Inhibitor Studies. In all experiments using pCMBS, LUV or ghosts were preincubated for 15–25 min with 1 mM pCMBS. Solutions of pCMBS were prepared immediately before use; care was taken to minimize exposure of the compound to light. In experiments using $HgCl_2$, vesicles or ghosts were preincubated 5–10 min in 1 mM $HgCl_2$. In experiments using cytochalasin B, vesicles or ghosts were preincubated 20 min in 10 μM cytochalasin B; the same concentration of cytochalasin was present in solutions in both drive syringes.

Analytical Procedures. ELISA was performed using C- and/or δ-IgGs as described by Carruthers and Helgerson (1989). Protein was determined by a modified Lowry procedure (Carruthers & Helgerson, 1989). Phospholipid phosphorus was determined by a modified Bartlett procedure (Carruthers & Melchior, 1984). [^{3}H]Cytochalasin B binding to reconstituted Glut1 was determined as described by Helgerson and Carruthers (1987). SDS–PAGE of membrane proteins and Glut1 was as described previously (Carruthers & Helgerson, 1989). Immunoblotting (Western) of proteins of δ- or C-antisera was as described in Harrison et al. (1990).

Statisical Methods. Means of experimental groups were compared using unpaired "t" tests; p values less than or equal to 0.05 were considered significant. To determine the statistical significance of a curve fit for a given set of data,

analysis of variance was performed. F values were determined:

$$F = \text{regression mean square/residual mean square} \quad (2)$$

with degrees of freedom calculated from the number of data points (400 per curve) and the number of independent variables in the curve fit eq 3. F values resulted in p values for all fitted curves which were <0.01 (Snedecor & Cochran, 1978).

Results

Glucose Fluxes in LUV. LUV were prepared with protein-free, lipid extracts of purified glucose carrier (lipid LUV), with reconstituted glucose carrier (Glut1 LUV), or with sufficient extracted erythrocyte protein (ghost LUV) calculated to reconstitute glucose carrier activity to a degree similar to that obtained in the Glut1 LUV. In each preparation, vesicles appeared as spheres of uniform distribution with diameters ranging from 1 to 2.5 μm, as determined by phase-contrast microscopy and laser scattering. Diameters averaged (mean ± SE) 1.7 ± 0.3 μm for lipid LUV, 1.6 ± 0.1 μm for ghost LUV, and 1.8 ± 0.0 μm for Glut1 LUV (n = 4; no significant differences between groups). The encapsulated [^{14}C]inulin volumes of the three preparations were similar (values expressed as microliters of entrapped volume per micromole of egg phosphatidylcholine): lipid LUV averaged 13.6 ± 0.9; ghost LUV averaged 15.7 ± 1.3, and Glut1 LUV averaged 14.8 ± 2.2 (n = 3; no significant differences between groups). Since the volume expected from encapsulation within 2-μm-diameter vesicles at 100% efficiency is 39.4 μL/μmol of egg phosphatidylcholine, the vesicle preparation protocol encapsulates with high efficiency. Moreover, the three vesicle preparations were the same diameters and were formed at similar efficiencies.

To determine the orientation of glucose carriers within reconstituted vesicles, two methods using specific antibodies to two distinct domains of the carrier were used. In the first method, binding of antibodies to intact vesicles (Glut1 LUV and ghost LUV) was compared with binding to a similar amount of pure carrier in solution (the appropriate amount of pure carrier in solution was determined by Western blots of the vesicle fractions). In the second method, antibody binding to intact vesicles was compared to binding to vesicles solubilized with Triton X-100. Using the first method, 47% and 49% of glucose carriers were oriented right-side-out in the Glut1 LUV and ghost LUV, respectively. Using the second method, these values were 50 and 51%, respectively. These results demonstrate that glucose carriers displayed equal tendencies to orient right-side-out and inside-out within the bilayer.

Figure 1 shows the uptake of α-D-[U-^{14}C]glucose in each of the LUV preparations. For ease of comparison, data are expressed as a percent of the encapsulated inulin space. Both ghost LUV and Glut1 LUV exhibited rapid uptake of glucose, achieving equilibrium values within 3 min. In both preparations, uptake was markedly inhibited with cytochalasin B. By contrast, glucose uptake in lipid LUV was much slower and was insensitive to cytochalasin B. Control experiments were performed to ensure that glucose carriers were evenly distributed through the LUV of the Glut1 LUV and ghost LUV preparations. Glucose uptake was measured at equilibrium in the absence (1 h) or presence (6 h) of cytochalasin B. Since the equilibrium values obtained in the presence of absence of cytochalasin were similar, functional glucose carriers were reconstituted into the entire population of LUV in each of these preparations.

Rate constants (k) for glucose uptake averaged (in s^{-1}; n = 3) (1.1 ± 0.1) × 10^{-3} for lipid LUV, (2.0 ± 0.1) × 10^{-2} for ghost LUV, and (1.6 ± 0.1 × 10^{-2} for Glut1 LUV. Equilibrium binding studies using [^{3}H]cytochalasin B gave maximum binding values of 102 and 119 nM for Glut1 LUV and ghost LUV, respectively. Assuming each carrier binds one molecule of cytochalasin B, these values translate into 1.15 × 10^{18} and 1.34 × 10^{18} carriers per liter of encapsulated volume in Glut1 LUV and ghost LUV, respectively. Assuming that the K_m for glucose of the carrier is 10 mM (Carruthers & Melchior, 1984), $V_{max} = kK_m$) values averaged 1.6 × 10^{-4} and 2.0 × 10^{-4} mol L^{-1} s^{-1} for Glut1 LUV and ghost LUV, respectively. From these values, the turnover number of the carriers (T_n; s^{-1}) was calculated. For Glut1 LUV, this value averaged 78 ± 5, while for ghost LUV this value averaged 98 ± 9. The calculated T_n for intact erythrocytes ranges from 158 to 792 (Carruthers, 1990). Tn for glucose and ghost LUV are similar to those reported previously and reflect some loss of activity when compared with values obtained in intact erythrocytes (Carruthers, 1990). The density of glucose carriers per unit membrane area was 25% of that of the intact erythrocyte.

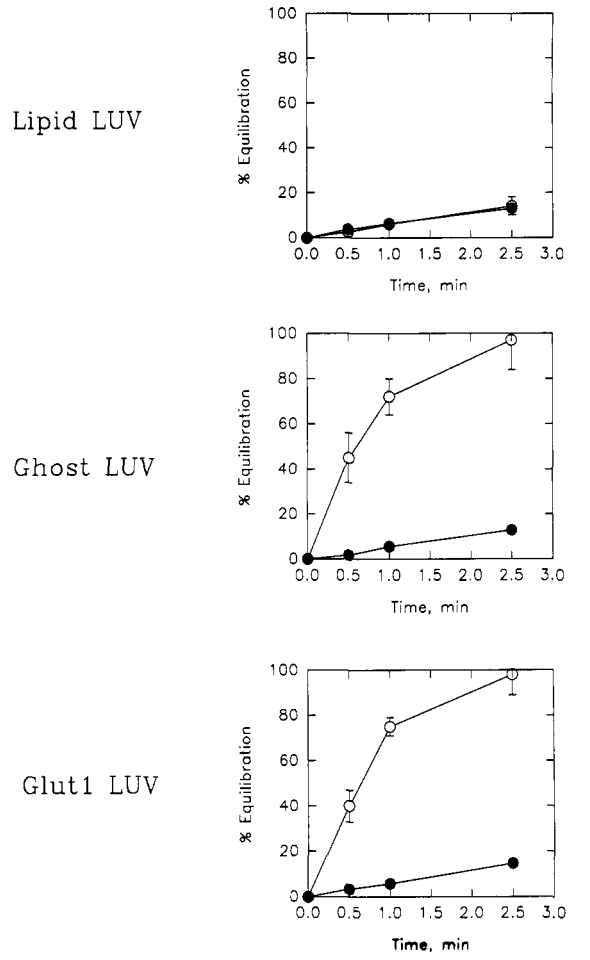

FIGURE 1: Glucose uptake in lipid LUV, ghost LUV, and Glut1 LUV. Time courses were performed in the absence (open circles) or presence (closed circles) of 10 μM cytochalasin B. Results are expressed as the percent equilibrium uptake and represent the mean ± SE for three preparations.

Water Flux in LUV. Figure 2 shows representative water flux tracings along with fitted single-exponential curves obtained in lipid LUV, ghost LUV, and Glut1 LUV. Data were fitted to single exponentials and the permeability coefficients calculated using vesicle diameters measured in each preparation. As shown in Table I, ghost LUV exhibited a 5–10-fold higher P_f than lipid LUV ($p < 0.01$); Glut1 LUV showed less of an increase, which did not achieve statistical significance ($p > 0.1$). Figure 2 also shows representative E_A determi-

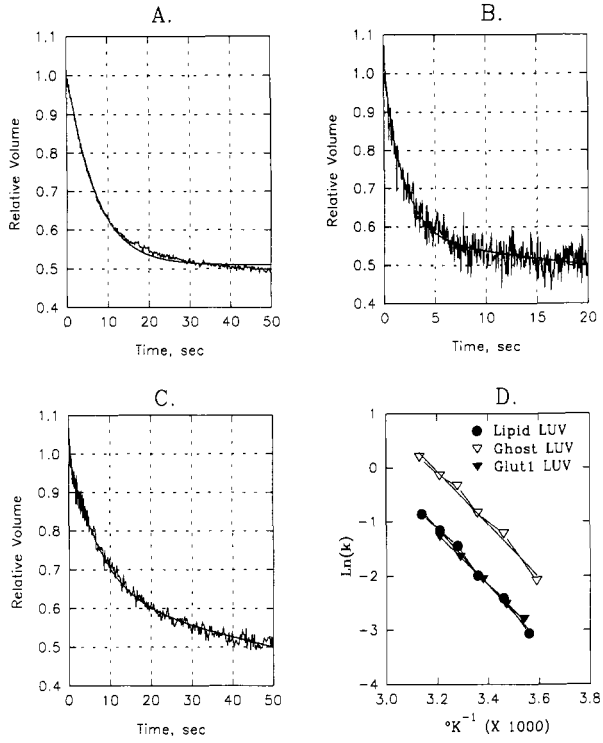

FIGURE 2: (Panels A–C) Water flux measurements in lipid LUV (panel A), ghost LUV (panel B), and Glut1 LUV (panel C). Vesicles loaded with 20 mM carboxyfluorescein were abruptly exposed to a doubling of extravesicular osmolality. Results are expressed as relative volume on the ordinate and time on the abscissa. Data and fitted curves are shown. (Panel D) Activation energies of water flux across the three vesicle preparations. Ordinate: Natural log of the rate constant, k, of the fitted exponential curve. Abscissa: $K^{-1} \times 1000$. In all panels, the data are representative of those obtained on at least four separate preparations.

Table I: Water Permeabilities, LUV Preparations ($n = 4$)[a]

	lipid LUV	ghost LUV	Glut1 LUV
P_f (cm/s)	0.0012 ± 0.0003	0.0060 ± 0.0014	0.0032 ± 0.0015
E_A (kcal/mol)	10.3 ± 0.1	10.1 ± 1.3	13.3 ± 2.4
effect of pCMBS (%)	+2.2 ± 17.5	+4.7 ± 1.1	+6.1 ± 20.0
effect of cyto B (%)	+0.1 ± 1.1	+0.8 ± 5.2	−12.5 ± 6.4

[a] All measurements except those of E_A were performed at 20 °C; results are expressed as mean ± SEM. Ghost LUV but not Glut1 LUV exhibited a statistically significant increase in P_f compared with lipid LUV.

nations; averages of these values are tabulated in Table I. Also summarized in Table I are the effects of pCMBS, $HgCl_2$, and cytochalasin B on P_f in each of the vesicle preparations.

These results demonstrate a significant ($p < 0.01$) increase in P_f over lipid LUV in ghost LUV. However, two other features of water channel activity, low activation energy and inhibition by organic mercurials, are not present. Although glucose transport in glucose and ghost LUV was inhibited by cytochalasin B, water flux was unchanged by this agent.

Flux Measurements in Erythrocyte Ghosts. As noted above, the turnover numbers of reconstituted glucose carriers are lower than those observed in intact erythrocytes and ghosts. Therefore, the apparent lack of water channel activity could be due to changes in the behavior of glucose carriers brought about by reconstitution. To approach this issue, erythrocyte ghosts with intact water channel and glucose carrier activities were prepared, and the effects of inhibition of glucose flux were examined. Figure 3 shows measurements of water permeability in freshly prepared human erythrocyte ghosts. Panels A–C depict representative tracings of relative volume as a function of time in the absence (panel A) or presence of

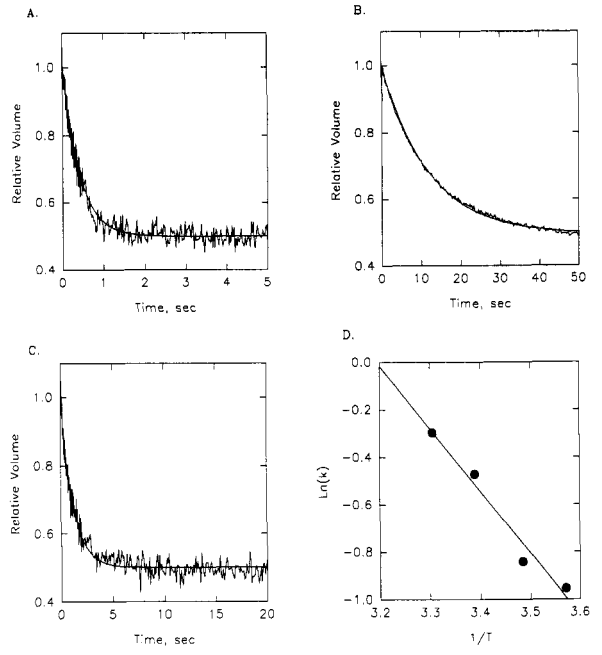

FIGURE 3: Water permeability of erythrocyte ghosts. (Panel A) Measurement in untreated ghosts. (Panel B) Effect of 1 mM $HgCl_2$; note the prolonged time scale. (Panel C) Effect of 1 mM pCMBS; note the prolonged time scale. (Panel D) Activation energy for water flow. These data are representative of similar results obtained in six to eight ghost preparations.

pCMBS (panel C) or mercuric chloride (panel B). Control P_f of 12 such preparations averaged 0.040 ± 0.009 cm/s (SEM), a value in good agreement with values previously obtained in intact erythrocytes (Macey, 1984; Solomon, 1972; Finkelstein, 1986). Inhibition of water flow by pCMBS averaged 63% (P_f = 0.015 ± 0.006 cm/s). Exposure to mercuric chloride reduced water flow by 85% (P_f = 0.0059 ± 0.0032 cm/s). Panel D shows a representative activation energy (E_A) determination. E_A for six ghost preparations averaged 3.6 ± 0.4 kcal/mol; R values for E_A plots were greater than 0.95. These data indicate that the ghosts used in the present study retained functional water channels.

Two approaches were used to determine whether water flux across the ghost membrane was mediated by the glucose carrier. Since exposure to calcium during ghost preparation inhibits glucose flux by over 95% (Helgerson et al., 1989), ghosts were prepared in the presence and absence of calcium and water and glucose fluxes measured. In addition, the effects of cytochalasin B on water and glucose fluxes were examined in ghosts prepared in the absence of calcium. Glucose fluxes in ghosts prepared in the absence of calcium averaged 12.8 ± 3.5 μmol L^{-1} min^{-1} (n = 3). By contrast, cytochalasin B inhibitable glucose flux in ghosts prepared in the presence of calcium was not detectable in three preparations. Figure 4 compares water fluxes in ghosts prepared in the presence and absence of calcium. P_f averaged 0.044 ± 0.009 cm/s in calcium-free ghosts in 0.038 ± 0.013 cm/s in ghosts prepared with calcium; these values were not significantly different. The effect of cytochalasin B was examined in ghosts prepared in the absence of calcium. In eight preparations, P_f averaged 0.044 ± 0.009 cm/s in the absence and 0.045 ± 0.014 cm/s in the presence of cytochalasin B; these values were not significantly different. Examination of glucose fluxes in the same ghost preparations revealed that cytochalasin B inhibited glucose uptake by over 95%.

Discussion

Water flux across erythrocyte membranes exhibits several

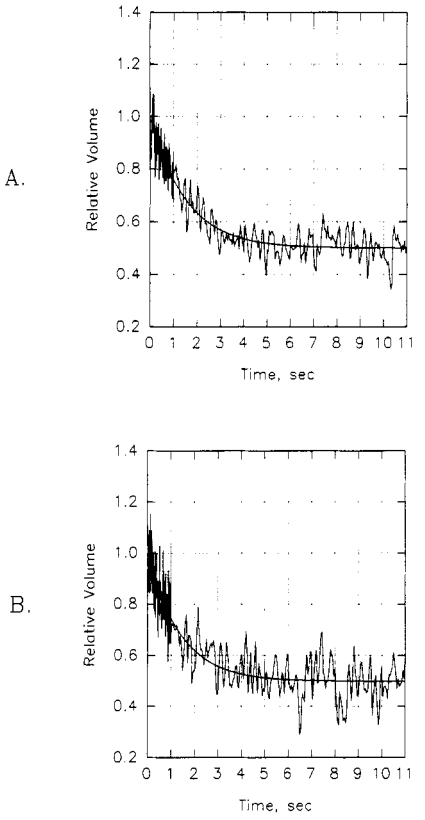

FIGURE 4: Effect of calcium on erythrocyte ghost water flow. Ghosts were prepared in an identical fashion in the presence (panel A) or absence (panel B) of calcium, and water flux was measured.

characteristics of flux via pores or water channels (Macey, 1984; Finkelstein, 1986). Thus, erythrocyte water permeability is high and is inhibitable with organic mercurial reagents like $HgCl_2$ and pCMBS. In addition, water flux exhibits an activation energy of 3–4 kcal/mol, a value similar to that of water diffusion through aqueous medium. Finally, the ratio of diffusive to osmotic water permeability is markedly greater than 1. By all of these biophysical criteria, water crosses the erythrocyte membrane via pores or channels, and these criteria have been used to identify functional water channels in erythrocyte preparations as well as other tissues (Macey, 1984; Harris et al., 1991). However, the identity of these water channels remains unknown. Calculations of water channel density which are based on the permeability of the erythrocyte membrane and the expected permeability of an individual channel (assuming that each channel has a permeability similar to that of the gramicidin channel) predict that there are 10^6 water channels per erythrocyte (Finkelstein, 1986). These considerations suggest that water channel proteins are abundant in erythrocytes, particularly if the channel is a dimer of multimer (Macey, 1984; Finkelstein, 1986).

The two most abundant erythrocyte membrane transport proteins are the anion exchanger and the glucose carrier (Macey, 1984; Finkelstein, 1986). Initially, the anion exchanger proved an attractive candidate for mediating water flux (Solomon, 1972). However, inhibition of water flux with pCMBS did not reduce anion exchange, and stilbenes inhibited anion exchange without altering water flux (Macey, 1984; Finkelstein, 1986). In addition, avian erythrocytes exhibit anion exchange similar to that observed in mammals without detectable water channel function (Macey, 1984).

Recently it has been suggested that glucose carriers may function as water channels (Fischbarg et el., 1989; 1990). Infrared spectroscopy of reconstituted glucose carriers has provided suggestive evidence that a large proportion of the protein is accessible to deuterium for exchange, consistent with the presence of a pore capable of conducting water (Alvarez et al., 1987; Jung et al., 1986). Measurements of osmotic water flow in J774 macrophages have demonstrated that inhibitors of mediated glucose transport such as cytochalasin B, tometin, and phloretin, but not the inactive dihydrocytochalasin B, reduce water flow with a potency similar to that obtained in measurements of glucose flux (Fischbarg et al., 1989). Injection of glucose transporter mRNA into *Xenopus* oocytes results in increased water permeability which appears to be inhibitable by cytochalasin B (Fischbarg et al., 1990). In light of these observations, it has been suggested that the erythrocyte glucose carrier may in fact function as the water channel (Fischbarg et al., 1990). In support of this view, pCMBS inhibits both water and glucose flux (Macey, 1894; Finkelstein, 1986; Carruthers, 1990). In addition, avian erythrocytes lack both water channels and significant sugar transport activity (Macey, 1984; Carruthers, 1990). Extrapolations from the oocyte data suggest that the increment in water permeability observed in oocytes expressing glucose carriers would be sufficient to account for erythrocyte water permeability given the number of glucose carriers per erythrocyte (Fischbarg et al., 1990).

The present studies were designed to test the hypothesis that the glucose carrier functions as the erythrocyte water channel. An attractive feature of this hypothesis is the wealth of knowledge of glucose carrier structure and function (Carruthers, 1990). The carrier can be reconstituted in a variety of lipid milieus, and its kinetic features are well characterized. In addition, several classes of glucose carrier have been identified and cloned, allowing potential application of structural information to an understanding of water channel function (Carruthers, 1990). To test whether glucose carriers function as water channels, we used two general approaches: We constituted glucose carriers into proteoliposomes at high density and examined the effects of these proteins on water flux. In addition, we examined the effects of inhibitors of glucose carrier function on water flux in erythrocyte ghosts with preserved water channel function.

It is clear from Figure 1 that vesicles incorporating mixed ghost proteins or purified glucose carrier exhibited classic glucose carrier function. The cytochalasin binding data reveal that the density of glucose carriers in the ghost and glucose liposomes approached that observed in intact erythrocytes. The reasons for the decreased apparent turnover number of reconstituted carriers when compared with carriers in intact erythrocytes remain unclear, but this low turnover number has been a consistent feature of all reported preparations of reconstituted erythrocyte glucose carrier (Carruthers, 1990).

Ghost LUV exhibited higher P_f values than those obtained in lipid LUV; the P_f in ghost LUV approached that obtained in intact erythrocytes. However, the increase in water permeability was not accompanied by reconstitution of the biophysical properties of native water channels. Thus, the activation energies of all preparations remained greater than 10 kcal/mol, and there was no demonstrable sensitivity of the observed water flow to mercurial reagents. These results are consistent with earlier reports which showed that reconstitution of erythrocyte proteins into liposomes increased water permeability (Carruthers & Melchior, 1984) and suggest that water flux was not occurring via channels. Rather the introduction of protein into the membrane appears to have increased the "leak" of water across the lipid bilayer [see Carruthers and Melchior (1984)]. The fact that water flow

increased more in the ghost LUV than in the Glut1 LUV, despite incorporation of similar densities of glucose carriers, adds further evidence that it is the presence of membrane proteins rather than glucose carriers that increases water premeability.

This conclusion is supported by calculation of the permeability of individual Glut1 carriers or protein molecules (p_f), assuming that the increment in water flux in ghost LUV (P_f of ghost LUV minus that of lipid LUV, 0.005 ± 0.0014 cm/s) is due entirely to reconstituted Glut1 or to nonspecific proteins: If we assume that all of the increment in P_f in ghost LUV was caused by reconstitution of Glut1 carriers, then 100 μg of Glut1 per 30 mg of egg PC results in 3×10^{10} Glut1 carriers/cm^2. The permeability of each carrier is then determined as

$$P_f = P_f(\text{cm/s})/\text{carrier density(carriers/cm}^3) = (16.7 \pm 4.9) \times 10^{-14}\ \text{cm}^3/\text{s} \quad (3)$$

This value is more than 5 times that of the gramicidin water channel (3×10^{-14} cm^3/s) and thus appears unreasonably high. If we make similar assumptions regarding Glut1 LUV, the increment in P_f caused by insertion of Glut1 carriers is at most 0.002 ± 0.0018 cm/s, and the corresponding p_f for these carriers is at most $(6.7 \pm 6.0) \times 10^{-14}$ cm^3/s, a value less than half that of the ghost LUV value. Thus, despite the identical activities of glucose uptake in ghost LUV and Glut1 LUV, the increments in water permeabilities do not predict similar p_f values for Glut1 in both preparations.

If, by contrast, we assume that all of the protein participates in the increase in P_f of the ghost LUV over the lipid LUV, these calculations are as follows: Since half of the total ghost protein is integral membrane protein and 90% of this is present in band 3 with a molecular mass of 95 kDa, 2.5 mg of protein was reconstituted per 30 mg of egg PC, resulting in a protein density in the membrane of 3×10^{11} protein molecules/cm^2. Then the "permeability" of individual protein molecules is $p_f = (1.7 \pm 0.5) \times 10^{-14}$ cm^3/s. This value is half that of the gramicidin water channel and appears more realistic. These calculations agree with the qualitative conclusion stated above that it is the incorporation of protein rather than the reconstitution of Glut1 carriers that increases P_f of ghost LUV over P_f of lipid LUV.

Because reconstituted glucose carriers exhibit reduced turnover numbers, it remained possible that the water channel activity of the carrier was also markedly reduced during reconstitution. We therefore prepared ghosts with intact water channels and examined the effects on water flow of perturbations in the glucose carrier. Previous studies using ghosts have revealed varying sensitivities of water flux to pCMBS, indicating that details of ghost preparations determine the preservation of water channel function (Ojcius et al., 1988). In our preparation, P_f was normal, sensitivity to mercurials was retained, and the E_A was below 5 kcal/mol, all indicators of retention of water channel function. In ghosts with preserved water channel function, two maneuvers which markedly inhibited carrier-mediated glucose flux, preparation of the ghosts in the presence of calcium and exposure to cytochalasin B, did not appreciably alter P_f.

Our method for measuring osmotic water flux in erythrocyte ghosts offers several advantages over previous techniques which depended on light scattering (Ojcius et al., 1988). First, the use of entrapped fluorescein markedly increases the signal and reduces the amount of ghost membrane needed for permeability measurements; in our studies, only 5–6 mL of blood was needed per ghost preparation. Second, the relationship between relative fluorescence and relative volume is more direct when fluorescein quenching is used as an indicator of relative volume.

Taken together, our results demonstrate that the incorporation of membrane transport proteins into liposomes can increase water permeability and suggest that this increase is due to nonspecific interactions between protein and lipid molecules. While it is possible that water can cross the membrane via the glucose carrier, it appears that this pathway does not account for the bulk of water flux across the membrane of the intact erythrocyte. The protein(s) and possibly protein/lipid complexes which make up the erythrocyte water channel remain elusive. Successful efforts to reconstitute functional water channels must include the demonstration of increased water permeability as well as evidence that biophysical characteristics of water channel function (such as low E_A and sensitivity to mercurial reagents in the case of erythrocyte water channels) are preserved.

Acknowledgments

We thank A. K. Solomon, H. W. Harris, J. Fischbarg, and S. Silverstein for helpful discussions.

Registry No. Water, 7732-18-5; glucose, 50-99-7; calcium, 7440-70-2.

References

Alvarez, J., Lee, D. C., Baldwin, S. A., & Chapman, D. (1987) *J. Biol. Chem. 262*, 3502–3509.

Benga, G., Pop, V. I., Popescu, O., Ionescu, M., & Mihele, V. (1983) *J. Membr. Biol. 76*, 129–137.

Benga, G., Popescu, O., Pop, V. I., & Holmes, R. P. (1986) *Biochemistry 25*, 1535–1538.

Bevingtons, P. R. (1969) *Data Reduction and Error Analysis for the Physical Sciences*, McGraw-Hill, New York.

Cairns, M. T., Elliot, D. A., Scudder, P. R., & Baldwin, S. A. (1984) *Biochem. J. 221*, 179–188.

Carruthers, A. (1986) *Biochemistry 25*, 3592–3602.

Carruthers, A. (1990) *Physiol. Rev. 70*, 1135–1176.

Carruthers, A., & Melchior, D. L. (1983) *Biochemistry 22*, 5797–5807.

Carruthers, A., & Melchior, D. L. (1984) *Biochemistry 23*, 6901–6911.

Carruthers, A., & Helgerson, A. L. (1989) *Biochemistry 28*, 8337–8346.

Chen, P.-Y., Pearce, D., & Verkman, A. S. (1988) *Biochemistry 27*, 5713–5718.

Finkelstein, A. (1986) *Water movement through lipid bilayers, pores and plasma membranes, theory and reality*, Wiley and Sons, New York.

Fischbarg, J., Kuang, K., Hirsch, J., Lecuona, S., Rogozinski, L., Silverstein, S. C., & Loike, J. (1989) *Proc. Natl. Acad. Sci. U.S.A. 86*, 8397–8401.

Fischbarg, J., Kuang, K., Vera, J. C., Arant, S., Silverstein, S. C., Loike, J., & Rosen, O. M. (1990) *Proc. Natl. Acad. Sci. U.S.A. 87*, 3244–3247.

Harris, H. W., Handler, J. S., & Blumenthal, R. (1990a) *Am. J. Physiol. 258*; F237–F243.

Harris, H. W., Kikeri, D., Janoshazi, A., Solomon, A. K., & Zeidel, M. L. (1990b) *Am. J. Physiol. 259*, F366–F371.

Harris, H. W., Strange, K., & Zeidel, M. L. (1991) *J. Clin. Invest. 88*, 1–8.

Harrison, S. A., Buxton, J. M., Helgerson, A. L., MacDonald, R. G., Chlapowski, F. J., Carruthers, A., & Czech, M. P. (1990) *J. Biol. Chem. 265*, 5793–5801.

Hebert, D. N., & Carruthers, A. (1991) *Biochemistry 30*, 4654–4658.

Helgerson, A. L., & Carruthers, A. (1987) *J. Biol. Chem. 262*, 5464-5475.
Helgerson, A. L., Hebert, D. N., Naderi, S., & Carruthers, A. (1989) *Biochemistry 28*, 6410-6417.
Illsley, N. P., & Verkman, A. S. (1986) *J. Membr. Biol. 94*, 267-278.
Jung, E. K. Y., Chin, J. J., & Jung, C. Y. (1986) *J. Biol. Chem. 261*, 9155-9160.
Macey, R. I. (1984) *Am. J. Physiol. 246*, C195-C203.
Meyer, M. M., & Verkman, A. S. (1986) *Am. J. Physiol. 251*, C549-C557.
Ojcius, D. M., Toon, M. R., & Solomon, A. K. (1988) *Biochim. Biophys. Acta 944*, 19-28.
Snedecor, G. W., & Cochran, W. G. (1978) *Statistical Methods*, Iowa State University Press, Iowa City, IA.
Solomon, A. K. (1972) in *Biomembranes* (Kreuzer, F., & Slegers, J. F. G., Eds.) pp 299-330, Plenum Publishing Corp., New York.

Biphasic Changes in the Level and Composition of *Dunaliella salina* Plasma Membrane Diacylglycerols following Hypoosmotic Shock†

Kwon-Soo Ha and Guy A. Thompson, Jr.*
Department of Botany, University of Texas, Austin, Texas 78713
Received July 18, 1991; Revised Manuscript Received September 26, 1991

ABSTRACT: Hypoosmotic shock has been shown to trigger an immediate and selective increase of plasma membrane diacylglycerols (DAG) in the green alga *Dunaliella salina*, coinciding with an approximately equivalent loss of phosphatidylinositol 4,5-bisphosphate from this membrane [Ha, K. S., & Thompson, G. A., Jr. (1991) *Plant Physiol. 97*, 921-927]. Following a slight decline in amount, DAG levels of the plasma membrane resumed their rise by 2 min after the shock and by 40 min had achieved a maximum concentration equivalent to 230% of DAG levels in unstressed cells. This second, more sustained increase of plasma membrane DAG was matched by a DAG increase in the microsome-enriched cytoplasmic membrane fraction, commencing at 2 min and peaking at 140% of control values. The changing pattern of DAG molecular species produced in the plasma membrane during the early phases of hypoosmotic stress was compatible with their derivation from phospholipase C hydrolysis of inositol phospholipids and phosphatidylcholine. From 8 min following hypoosmotic shock, as relatively larger scale DAG accumulations developed in the cytoplasmic membranes, the molecular species composition changed to reflect a marked increase in de novo synthesis of *sn*-1-oleoyl, *sn*-2-palmitoylglycerol, and dioleoylglycerol. The former molecular species appears to be synthesized in the chloroplast while the latter is produced in the endoplasmic reticulum. The radioisotope labeling data with $Na_2{}^{14}CO_3$ confirmed that the biphasic formation of DAG triggered by hypoosmotic shock culminates in a large-scale de novo synthesis of DAG. This is the first clear evidence for de novo synthesis as a source of DAG following PIP_2-mediated signaling. Cells briefly preincubated with [^{32}P]P_i sustained a more pronounced labeling of an approximately 29-kDa protein during the first 30 s following hypoosmotic shock than did nonstressed cells during the same time period. The difference in labeling intensity between stressed and nonstressed cells was less marked during the second phase of DAG production.

Transmembrane signaling via the phospholipase C mediated hydrolysis of phosphatidylinositol 4,5-bisphosphate (PIP_2)[1] has been implicated in the activation of many cell types by external agonists and environmental stresses (Guy et al., 1989). We have shown this pathway to be triggered in the green alga *Dunaliella salina* by hypoosmotic stress (Einspahr et al., 1988; Ha & Thompson, 1991). A rapid increase in diacylglycerols (DAG), known to act as second messengers in this signaling pathway, occurred selectively in the plasma membrane during the brief period of maximal PIP_2 hydrolysis, and the principal molecular species of DAG which increased in amount there were characteristic of those predominating in inositol-containing phospholipids only (Ha & Thompson, 1991). The sudden stress-induced rise in *D. salina* DAG was superimposed on a significantly higher basal level of DAG than is generally found in animal cells. Those higher plants which have been analyzed (Morré et al., 1989; Morse et al., 1987) also contain relatively higher concentrations of DAG, raising the interesting question of how these systems discriminate between "signaling" and "non-signaling" DAG.

When quantitative analysis of the hypoosmotic shock-induced DAG content was extended to longer time periods, it became clear that a second, more pronounced phase of DAG production closely followed the first phase. In this respect, DAG kinetics in *D. salina* closely resemble those observed in a number of animal cell systems (Fukami & Takamura, 1989; Matozaki & Williams, 1989; Cook et al., 1990; Pessin et al., 1990). The present paper examines the composition, the intracellular location, and the metabolic sources of DAG arising

† This work was supported in part by NSF Grant DCB-8802838 and Welch Foundation Grant F-350.

[1] Abbreviations: DAG, diacylglycerol(s); PC, phosphatidylcholine; PI, phosphatidylinositol; PIP_2, phosphatidylinositol 4,5-bisphosphate; PL, phospholipid; PKC, protein kinase C; in the shorthand numbering system used to identify fatty acids, the number preceding the colon indicates the number of carbon atoms and that following the colon the number of double bonds present; pairs of numbers designating fatty acids in this way, when placed before and after a slash, represent the components in the *sn*-1 and *sn*-2 positions, respectively, of a lipid molecular species.

0006-2960/92/0431-596$03.00/0